Dynamic deformability of *Plasmodium falciparum*-infected erythrocytes exposed to artesunate *in vitro*†

Sha Huang,‡[a] Andreas Undisz,‡§[b] Monica Diez-Silva,[b] Hansen Bow,[a] Ming Dao*[b] and Jongyoon Han*[ac]

Artesunate (ART) is widely used for the treatment of malaria, but the mechanisms of its effects on parasitized red blood cells (RBCs) are not fully understood. We investigated ART's influence on the dynamic deformability of ring-stage *Plasmodium falciparum* infected red blood cells (iRBCs) in order to elucidate its role in cellular mechanobiology. The dynamic deformability of RBCs was measured by passing them through a microfluidic device with repeated bottleneck structures. The quasi-static deformability measurement was performed using micropipette aspiration. After ART treatment, microfluidic experiments showed 50% decrease in iRBC transit velocity whereas only small (∼10%) velocity reduction was observed among uninfected RBCs (uRBCs). Micropipette aspiration also revealed ART-induced stiffening in RBC membranes. These results demonstrate, for the first time, that ART reduces the dynamic and quasi-static RBC deformability, which may subsequently influence blood circulation through the microvasculature and spleen cordal meshwork, thus adding a new aspect to artesunate's mechanism of action.

Insight, innovation, integration

Artemisinin is an important drug for malaria treatment, but its mechanism remains unclear. Past studies largely focused on the biochemistry of artemisinin to explain its mechanism. In this paper, ART (artemisinin derivative)-induced change in RBC membrane stiffness is investigated by passing RBCs through a microfluidic device that mimics and simulates splenic filtration and other *in vivo* RBC deformations during microcirculation. After ART treatment, the membrane stiffness of both uninfected and infected RBCs increases moderately (∼10%), corresponding to a significant decrease in RBC transit velocities. Our result suggests that drug-induced RBC stiffening could significantly alter blood circulation and enhance the efficiency and specificity of splenic parasite clearance, elucidating a previously unexplored, mechanical aspect of the artemisinin drug mechanism.

Introduction

Malaria is the most deadly parasitic disease which affects 200 million people worldwide and accounts for nearly one million annual deaths.[1] The most virulent malarial parasite *Plasmodium falciparum* can lead to severe complications and has the highest mortality rate.[2] During its asexual stage, *P. falciparum* infects red blood cells (RBCs), which then undergo notable morphological and rheological changes from the ring stage to the trophozoite and finally the schizont stage, constituting a 48 h asexual reproduction cycle.[3] Cyclic febrile attack is a characteristic clinical feature of *P. falciparum* malaria, which corresponds to the release of merozoites in circulation following infected RBCs (iRBC) rupture in the late schizont stage.

Apart from cerebral malaria, malarial anemia is the most frequent and severe syndrome of *falciparum* malaria.[4] Massive loss of RBCs cannot be entirely attributed to the destruction of iRBCs, which usually constitute only a small fraction of total RBCs in malaria patients. Instead, the major cause of malarial anemia is believed to be the excessive loss of *uninfected* RBCs (uRBCs),

[a] *Department of Electrical Engineering and Computer Science, Massachusetts Institute of Technology, 77 Massachusetts Avenue, Cambridge, MA 02139, USA. E-mail: jyhan@mit.edu*
[b] *Department of Materials Science and Engineering, Massachusetts Institute of Technology, 77 Massachusetts Avenue, Cambridge, MA 02139, USA. E-mail: mingdao@mit.edu*
[c] *Department of Biological Engineering, Massachusetts Institute of Technology, 77 Massachusetts Avenue, Cambridge, MA 02139, USA*
† Electronic supplementary information (ESI) available. See DOI: 10.1039/c2ib20161e
‡ These authors contributed equally to this work.
§ Current address: Department of Metallic Materials, Friedrich-Schiller-University, Loebdergraben 32, 07743 Jena, Germany.

mostly in the spleen and/or the liver.[5] Malaria-related dyserythro-poiesis is likely a minor factor because complete removal of erythro-poiesis brings about only a minor decrease in RBC population.[6] On the other hand, it has been suggested that uRBCs exposed to the parasites are slightly less deformable, and/or decorated with parasite molecules,[7] both of which could potentially lead to splenic retention and clearance of a large number of uRBCs, exacerbating malarial anemia. However, the exact causes and mechanisms of malarial anemia are yet to be firmly established.

Several studies indicate that RBC filtration in the spleen is critical to influencing diverse pathophysiological outcomes of malaria.[8] Splenomegaly (enlarged spleen) is a clinical consequence of malaria infection. The narrow splenic inter-endothelial slits (~1–2 μm in height) provide a stringent mechanical filter through which only RBCs with adequate deformability can pass. In the later (trophozoite and schizont) stages of malaria, iRBCs can be up to 50 times stiffer than uRBCs.[9] However, in the earlier ring-stage (which occurs within the first 24 h of intra-erythrocytic invasion of the parasite), iRBCs are only moderately stiffer than uRBCs. Although the ring stage is the only asexual parasite stage that can be found in blood circulation, a substantial (~50%) proportion of the ring-stage iRBCs are retained by the human spleen, as demonstrated in the experiment using isolated human spleens.[10] The Ring-infected Erythrocyte Surface Antigen (RESA) is one of the parasite-derived proteins responsible for the reduction of ring-stage iRBC membrane deformability.[11]

Clinical studies show that malaria patients with artesunate (ART) treatment exhibit a more rapid decline in the parasitemia and also that the accelerated parasite clearance is delayed in splenectomized patients.[12] The involvement of spleen is there-fore believed to be responsible for rapid parasite clearance after ART drug treatment.[5] The in vivo parasite clearance following ART treatment has often been attributed to a process known as 'pitting', whereby spleen removes intraerythrocytic parasites without destructing the host RBCs.[13,14] However, it is unclear whether pitting is the main mechanism of splenic parasite clearance. Studies by Newton et al. noted that the average lifespan of pitted RBCs (i.e. RESA-RBC) is only 183 hours, significantly shorter compared to the normal RBC life span of 1027 hours.[15] Furthermore, ART treatment was found to further shorten the pitted RBC life span, suggesting that other mechanisms facili-tating splenic parasite clearance may exist. Since spleen is also known as a "mechanical filter" that removes old and stiffened RBCs from microcirculation,[5,16] the rapid splenic parasite clear-ance after ART treatment might be attributed to ART altering the mechanical properties of iRBCs and possibly of uRBCs. However, there is currently a lack of experimental evidence to confirm such an effect of ART on RBC deformability.[14]

Experiments show that subtle changes in RBC deformability may lead to a significant shift in splenic RBC retention efficiency.[5,17] A sensitive single cell deformability cytometry for characterizing the dynamic deformability of both uRBCs and iRBCs is therefore essential for understanding malaria pathophysiology. Bulk cell measurements such as ektacytometry,[18,19] which describe the averaged values of RBC deformability through geometric esti-mates, do not provide reliable measures of individual cells'

mechanical properties. On the other hand, most of the established tools for single cell deformability measurements including micro-pipette aspiration,[20,21] atomic force microscopy,[22] and optical tweezers[11] require extensive experimental effort to extract reliable information for large populations of cells. More importantly, such measurements impose quasi-static loads to attain notable defor-mation, and the resulting information may not be directly applic-able to the more realistic situation involving dynamic cell deformation. Furthermore, static deformability of RBCs is char-acterized by the shear and bending moduli of the cell membrane, whereas dynamic deformability can be influenced by additional factors such as membrane viscosity and cell shape. When RBCs circulate in blood capillaries and spleen cordal meshwork, they undergo a complicated, time-dependent deformation process. Therefore, a more straightforward and direct way to evaluate the amenability of RBCs to pass through constrictions in the spleen and microcapillary blood vessels is to simulate such in vivo RBC deformations during circulation using microfluidic artificial filter structures.[23] In contrast to the conventional filtration system, in which the RBC "filterability" is evaluated directly by the percentage of cells that pass through, the microfluidic system employed in this work characterizes single RBC deformability via its transit velocity through repeated bottleneck structures while facilitating such measurements on a large population of cells.

In this paper, the influence of ART on RBC deformability in the pathology of P. falciparum malaria is evaluated using two approaches: a microfabricated deformability cytometer that mimics in vivo RBC microcirculation[24] and micropipette aspiration that measures RBC membrane stiffness. Besides, ART's effects on the mechanical properties of iRBCs were further assessed by treating the iRBCs in combination with pentoxifylline (PTX), a possible adjunctive therapy for cerebral malaria.[25–27]

## Materials and methods

Microfluidic device

The microfluidic device was designed with a layout program and it consists of 500 μm × 500 μm inlet/outlet reservoirs and parallel capillary channels with triangular pillar arrays (Fig. 1A). Two different inter-pillar gap sizes of 3.0 and 4.0 μm were tested for optimum deformation conditions. Detailed fabrication steps were described by Bow et al.[24]

Parasite culture

P. falciparum 3D7A parasites used in this study were obtained from Malaria Research and Reference Reagent Source, Amer-ican Type Culture Collection. Parasites were cultured as pre-viously described.[28] Cultures were synchronized at the ring stage by sorbitol lysis[29] two hours after merozoite invasion.

Artesunate drug treatment

The stock ART solution (1.25 mg ml^{-1}) was prepared by dissolving ART powder (Sigma A3731) in aqueous sodium bicarbonate. A highly synchronized culture of 6 hour old rings with ~15% parasitemia was resuspended at 0.1% hematocrit in malaria culture medium containing various concentrations of ART drug.
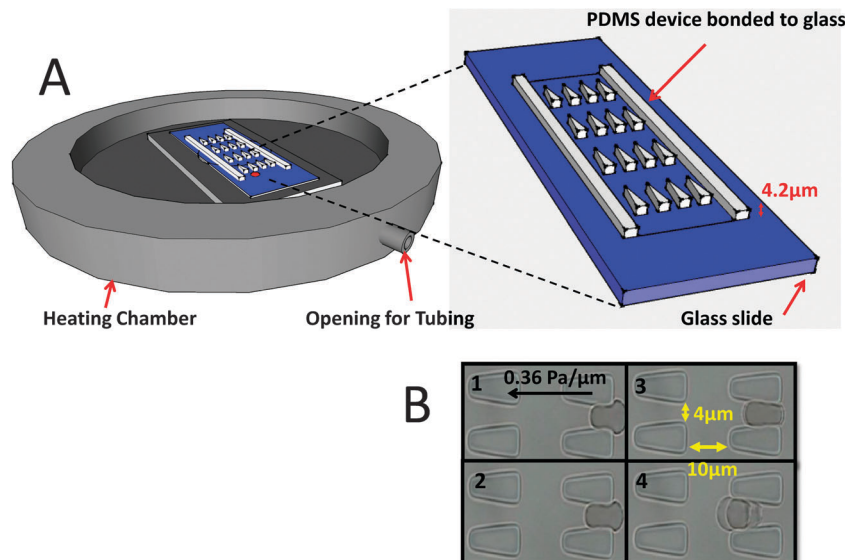
Fig. 1 Experimental schematics. (A) A heating chamber (Olympus) was mounted to the inverted microscope stage. The PDMS–glass bonded device consists of the inlet and outlet reservoirs and main channels with triangular pillar arrays. (B) Experimental images of uRBCs passing through the gaps.

In the control group, sodium bicarbonate solution without ART was added. Both drug and control groups were incubated at 37 °C for 2–6 h.

Solution preparation

Phosphate buffered saline (PBS) with 1% w/v Bovine Serum Albumin (BSA) (Sigma-Aldrich, St. Louis, MO) was freshly made on every experimental day as stock solution. For experiments measuring malaria infected cells, 1 ml of cultured cells were centrifuged at $350g$ for 5 min; 1 μl of the pellet was then aliquoted to 200 μl stock solution.

To distinguish infected cells from uninfected RBCs, 10 μl of 1×10^{-6} M thiazole orange (Invitrogen, Carlsbad, CA), which stains the RNA of the cell, was added to the aforementioned 200 μl iRBC containing solution 20 min before the experiment. The iRBCs would appear fluorescent under the GFP filter set whereas the uRBCs were seen as dark shadows.

Experimental protocol for microfluidics

To accurately control the ambient temperature, the microscope surface was replaced by a heating chamber (Olympus), which was preheated to a desired temperature for 30 min before the beginning of every experiment. Meanwhile, the PBS–BSA stock solution was injected into the device to coat the PDMS walls to prevent adhesion. This filling step need not be done inside the heating chamber, but the PBS–BSA filled device needed to be placed into the heating chamber at least 5 min before loading 5 μl of the diluted blood sample. During the temperature calibration phase, a thermocouple was used to probe the exact temperature inside the heating chamber. When the temperature needed to be adjusted to a different value, at least 5 min of waiting time was required to ensure a new stable ambient temperature.

The microfluidic device was driven by a constant pressure gradient across. The inlet reservoir was connected to a vertically held 60 ml syringe which was partially filled with the PBS–BSA buffer solution. A CCD camera (Hamamatsu Photonics, C4742-80-12AG, Japan) was connected to the inverted fluorescent microscope (Olympus IX71, Center Valley, PA) to capture the movement of the RBCs in the microchannels. Images were automatically acquired using IPLab (Scanalytics, Rockville, MD) at 100 ms time interval and the post-imaging analysis was done using imageJ. The velocity of individual RBCs was defined as the distance the cells moved divided by the time in seconds. To better illustrate drug-induced percentage change in iRBC/uRBC velocity, the term "normalized velocity" was adopted. Normalized velocity was obtained by dividing the measured velocity of individual RBCs under various experimental conditions by the average uRBC velocity of the control group on the same experimental day.

Experimental protocol for micropipette aspiration

Micropipette aspiration was carried out using an inverted optical microscope (Olympus IX71) equipped with a micromanipulator (Eppendorf Transferman NK 2), a heating stage (Linkam Scientific Instruments) and an objective heater (Tokai Hit thermoplate). Pipettes were drawn from borosilicate glass tubing (Sutter Instrument Model P-2000) and cut open (Narishige MF-900) prior to mounting to the micromanipulator. The pipette diameter was kept at 1.0 μm throughout the experiments. Prior to the measurements, the cell chamber was preheated to 37 °C and flushed with the PBS–BSA stock solution with the glass pipette readily mounted and inserted. After the temperature of the stock solution equalized to 37 °C, 1 μl of cells were injected into the cell chamber. Subsequently, the aspiration pressure was increased to 100 Pa at a rate of 0.5 Pa s^{-1} measuring one cell at a time. Images of each

aspirated cell were captured at a rate of 1 s^{-1} using a high-resolution digital camera (Olympus DP72). The maximum time span before the whole sample was replaced by a fresh sample was 1 h. From the high-resolution recordings, the leading edge of the aspired RBC membrane was tracked manually for calculating the elastic shear modulus using the spherical cap model.[21]

Statistical analysis

Two-tailed Student's *t*-tests were used to compare the micro-fluidic results and the shear modulus values under various test conditions.

Results

The microfluidic device comprises a series of equally spaced triangular pillar arrays with gap sizes ranging from 3 to 4 μm (Fig. 1 illustrates the system with 4 μm gap size). The gap sizes were designed to impose mechanical constraints similar to those encountered by the RBCs (with an average diameter of about 8 μm) when traversing blood capillaries and splenic meshwork. Driven by a constant pressure gradient that is smaller than the Pa μm^{-1} level, RBCs undergo large elastic deformation at each constriction while traversing the channel.[24] The dynamic deformability of RBCs is then characterized by their velocity at a given pressure gradient which signifies their ability to deform repeatedly in order to pass through many successive constrictions.

Fig. 1B presents sequential freeze-frame images of an uRBC moving inside the microchannel. The velocity of individual RBCs can then be derived by recording the time of passage of each cell through 10 constrictions in series (*i.e.* for a total travel distance of 200 μm). The typical pressure gradient ($\sim$0.5 Pa μm^{-1}) and shear rate ($\sim$100 s^{-1}) applied in this device as well as the resulting RBC flow rate (20–200 μm s^{-1}) are comparable to those of physiological flows;[30] they are also of the same order of magnitude as RBCs passing through splenic inter-endothelial slits (IES).[31]

Time-dependent effects of ART on the dynamic deformability of iRBCs

Ring-stage *P. falciparum* cultures were exposed to ART, an artemisinin derivative. The deformability of both iRBCs and co-cultured uRBCs was measured 2, 4 and 6 h after ART drug treatment. Cultures of iRBCs and uRBCs without ART treatment were used as control. All experiments were performed at 37 °C.

Fig. 2A demonstrates pronounced decrease in iRBC velocity after 4 h of ART exposure. Compared to the control iRBCs (40 μm s^{-1}), the average transit velocity of ART-exposed iRBCs was halved (20 μm s^{-1}), indicating a statistically significant reduction of the dynamic deformability induced by ART ($p < 0.001$). On the other hand, a much smaller decrease in the average transit velocity of uRBCs was observed after ART exposure.

To assess the time-dependent effects of ART treatment, the dynamic deformability measurements were performed after 2, 4,

and 6 h of ART exposure. The results are given in Fig. 2B and C. While no significant difference in the average iRBC velocity could be observed after 2 h ART incubation, iRBC velocity dropped significantly by approximately 40% after 4 h of ART exposure ($p < 0.001$).

The differential deformability between uRBCs and iRBCs was previously noted as the key parameter for efficient splenic filtration of iRBCs.[5,10,32,33] The deformability difference between uRBCs and iRBCs can be assessed through the index, R_s:

$$R_s = \frac{X_2 - X_1}{2(\sigma_1 + \sigma_2)}$$

Here X_1 and X_2 are the mean values of velocities of iRBCs and uRBCs, respectively, and σ_1 and σ_2 denote the standard deviations of velocities of iRBCs and uRBCs, respectively. A higher R_s value implies larger separation between the velocities of iRBCs and uRBCs.

While in both control and ART-exposed groups the iRBC velocities are significantly slower than that of co-cultured uRBCs ($p < 0.001$), the velocity separation resolution R_s was enhanced by 2.3 times from 0.33 to 0.77 after ART exposure. Additionally, the average iRBC velocity after ART exposure was 3.13σ_2 (σ_2: standard deviation of uRBC velocity distribution) away from the average uRBC velocity. This result suggests a more specific dynamic deformability differentiation between uRBCs and iRBCs after ART exposure, which may consequently lead to more efficient splenic parasite clearance.

Concentration-dependent ART effect on dynamic deformability of iRBCs

The *in vivo* serum concentration of ART varies with time after injection.[34,35] Typically, the half-life of ART in patients is approximately 3 h with a peak serum concentration of 0.1 μg ml^{-1}. Therefore, the dynamic deformability assay was further expanded to different concentrations. Fig. 2D indicates that from 0.01 μg ml^{-1} to 0.1 μg ml^{-1}, there is no statistically significant dose dependency on ART induced alteration of the RBCs deformability.

Time-dependent ART effect on the quasi-static deformability of iRBCs

In parallel with the microfluidic experiments, micropipette aspiration of iRBCs and uRBCs was carried out. The membrane elastic properties were determined before and after ART exposure of RBCs for 2, 4 and 6 h. As control, cultures of iRBCs and uRBCs without exposure to ART were measured. All measurements were performed at 37 °C.

Fig. 3 summarizes the membrane elastic shear moduli of uRBCs and iRBCs before and after exposure to ART. The mean values for the elastic shear moduli of the iRBCs were consistently 30% to 40% higher than the moduli of their uninfected counterparts. Solely after incubating with ART for 2 h, the mean elastic shear moduli for both iRBCs and uRBCs increased by 10% to 20% with a *p*-value of 0.06, which is approximately at the threshold level of statistical significance of $p = 0.05$.
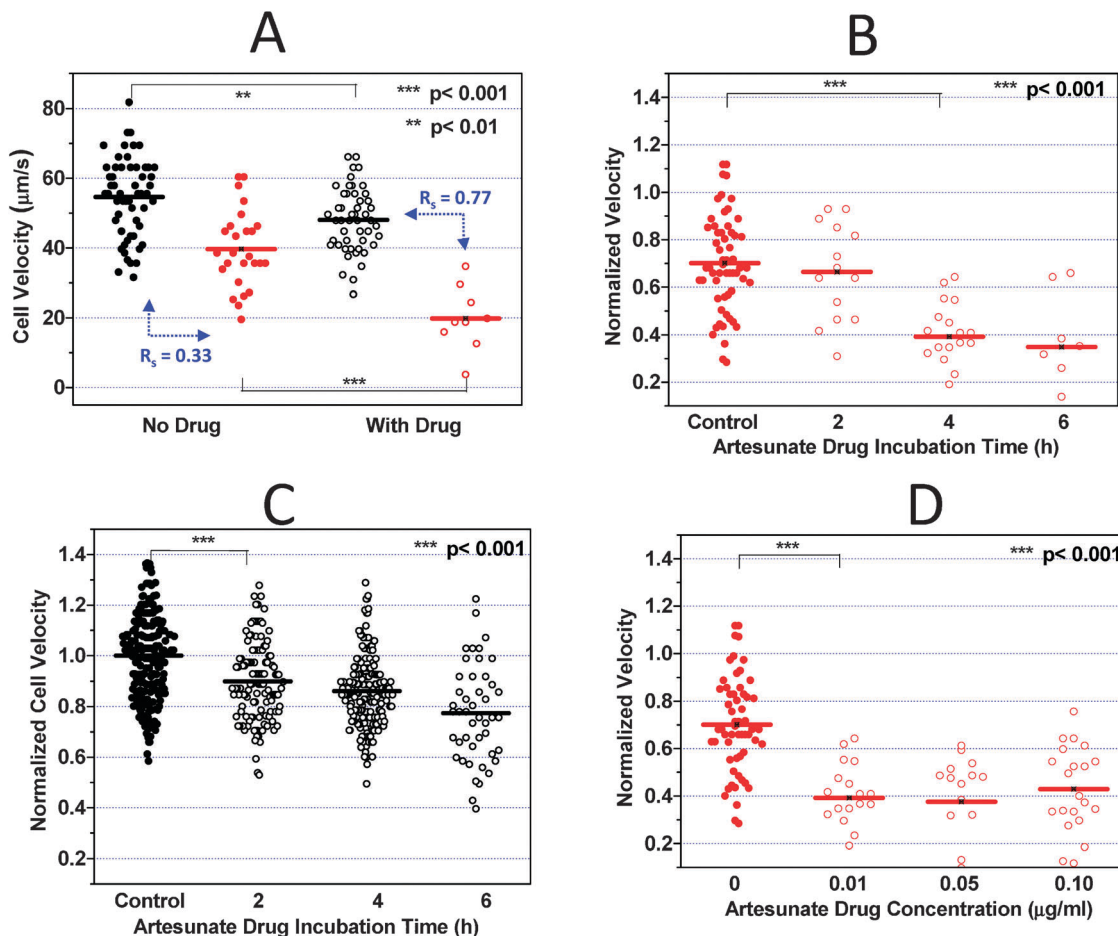
Fig. 2 Artesunate (ART) effect on iRBC/uRBC dynamic deformabilities. (A) 0.01 μg ml⁻¹ ART was added to the RPMI cell culture medium containing 0.1% hematocrit. After 4 h ART incubation, the iRBC velocities with and without ART treament were compared. (B) 0.01 μg ml⁻¹ ART was added to the RPMI cell culture medium containing 0.1% hematocrit. After 2, 4, and 6 h ART incubation, the iRBC velocities were compared. (C) Time dependent ART effects on uRBC velocities were studied. (D) 0.01, 0.05 and 0.10 μg ml⁻¹ ART was added to the RPMI cell culture medium containing 0.1% hematocrit. After 4 h ART incubation, the concentration dependent ART effects on iRBC velocities were compared. Black and red dots denote uRBCs and iRBCs without ART treatment whereas black and red circles denote uRBCs and iRBCs with ART treatment respectively. Velocity measurement on every experimental day is normalized against the average uRBC velocity in the control sample.

Exposure to ART results in an increase in the membrane elastic shear modulus of both uRBCs and iRBCs (Fig. 3). For uRBCs the relative increase in the mean elastic shear modulus is 20% ± 2% independent of the incubation time. For iRBCs the maximum relative increase was measured to be 20% after 4 h ART incubation.

### Effect of pentoxifylline on the dynamic deformability of iRBCs

Pentoxifylline (PTX), a hydroxyl radical scavenger,[19,36,37] is believed to be able to improve impaired blood flow. Several studies also suggest that it can be used as an ancillary treatment for severe *falciparum* malaria, in combination with ART. In this section, the effect of PTX alone, as well as the combined effect of PTX and ART on the dynamic deformability of *P. falciparum*-infected RBCs are studied *in vitro.* All experiments were performed at 37 °C.

Fig. 4A demonstrates that PTX has no statistically significant effect on the deformability of ring-stage iRBCs even after 4 h of incubation at a concentration of 100 μg ml⁻¹. The average transit velocity of iRBCs after PTX treatment was 33 μm s⁻¹,

which was very similar to that of the control sample (34 μm s⁻¹, $p = 0.54$). Simultaneous measurements were also performed on co-cultured uRBCs. Whereas the average uRBC velocity in the control sample was 43 μm s⁻¹, the value after PTX treatment was statistically different (46 μm s⁻¹, $p = 0.034$), exhibiting a significant albeit mild increase in the dynamic deformability of uRBCs.

The effect of PTX on the difference in response between uRBCs and iRBCs was calculated in a similar way as described before. The R_s value for the control sample was 0.33 compared to 0.40 after PTX treatment. The result suggests a marginal (if any) effect of PTX drug on RBC deformability.

Typical clinical dosage of PTX is between 5 and 20 μg ml⁻¹. To investigate whether the effect of PTX on uRBCs is dose-dependent, the co-cultured uRBCs were exposed to 20 μg ml⁻¹ and 100 μg ml⁻¹ PTX for 2 h. Compared to the control sample (42.79 μm s⁻¹), the average uRBC velocity exhibited significant improvement at both concentrations (52.03 μm s⁻¹ and 51.33 μm s⁻¹, $p < 0.01$) and no statistically significant concentration dependence could be concluded. Fig. 4B suggested that
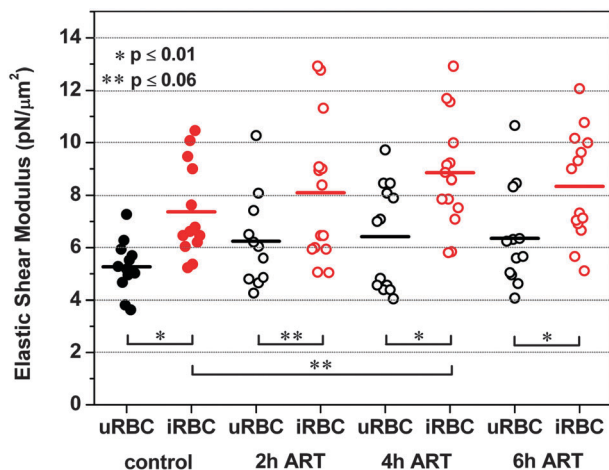
Fig. 3 Artesunate effect on iRBC/uRBC membrane stiffness. 0.05 µg ml^{-1} of ART were added to the RPMI cell culture medium containing 0.1% hematocrit. After 2, 4 and 6 h of incubation with ART, micropipette aspiration of uRBCs (black circles) and iRBCs (red circles) was carried out at a suction rate of 0.5 Pa s^{-1}. Black dots (uRBCs) and red dots (iRBCs) represent the control without ART treatment. The mean elastic shear moduli of the iRBCs are 30% to 40% higher than the moduli of their uninfected counterparts. Exposure to ART results in a mild but consistent increase in the membrane elastic shear modulus of both uRBCs and iRBCs.

the effect of PTX on uRBCs was not dose-dependent ($p = 0.67$) in the concentration range between 20 and 100 µg ml^{-1}.

After 2 h incubation with PTX, the uRBC dynamic deformability seemed to be slightly enhanced (from 42.79 to 52.03 µm s^{-1}). The effect remained for incubation up to 6 h (Fig. 4C). Simultaneous deformability measurement was obtained for iRBCs and no statistical significant effect was observed for up to 6 h PTX incubation (Fig. 4D).

The combined effect of PTX and ART is shown in Fig. 4E. Compared with ART only experiments, PTX does not seem to provide additional influences to the dynamic deformability of both iRBCs and uRBCs when applied in combination with ART.

Discussion

It is widely accepted that ring-stage *P. falciparum* parasites are the only asexual intra-erythrocytic parasite forms able to travel through human circulation without being recognized by the human host. Antimalarial drugs affecting ring-stage iRBC membrane mechanical properties would help the host with early identification of parasitized red blood cells, and consequently their effective clearance by the human spleen.
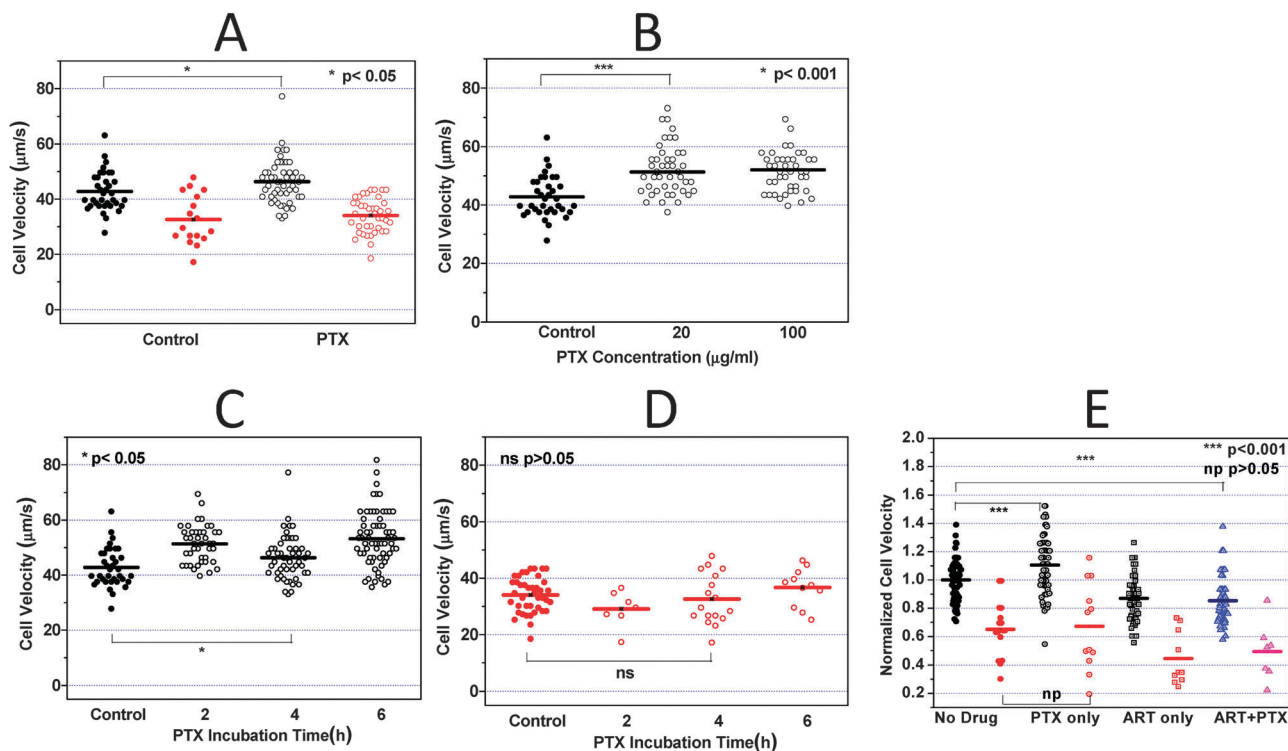
Fig. 4 Pentoxifylline (PTX) effect on iRBC/uRBC dynamic deformabilities. (A) 100 µg ml^{-1} PTX was added to the RPMI cell culture medium containing 0.1% hematocrit. After 2 h PTX incubation, the iRBC/uRBC velocities with and without PTX treatment were compared. (B) 20 and 100 µg ml^{-1} PTX was added to the RPMI cell culture medium containing 0.1% hematocrit. After 2 h PTX incubation, the velocities of uRBCs treated with different PTX concentrations were compared. (C) 100 µg ml^{-1} PTX was added to the RPMI cell culture medium containing 0.1% hematocrit. After 2, 4, and 6 h PTX incubation, the uRBC velocities under different test conditions were compared. (D) iRBC velocities after 2, 4 and 6 h PTX treatment were compared. No statistically significant change in iRBC velocity can be concluded. (E) PTX–ART combination effect on RBC deformability. No statistically significant difference can be concluded comparing RBCs treated with ART only *versus* cells treated with PTX–ART combinational therapy.

In the present study we explored the effect of two different drugs (artesunate and pentoxifylline) on the microcirculatory velocity of RBCs after malaria infection. Both drugs are used alone or in combination for the treatment of *P. falciparum* malaria: artesunate (ART) is known to facilitate splenic parasite clearance,[38] and pentoxifylline (PTX) has been suggested as an effective adjunctive therapy with ART,[39] but their relevant effects on the RBC mechanical properties are not yet well understood.

Our results demonstrate that ART treatment significantly stiffens ring-stage iRBCs based on both quasi-static and dynamic single cell deformability assays. Additionally, our microfluidic set up mimicking RBC microcirculatory behavior revealed that ART has a significant impact on the velocity separation resolution between iRBCs and uRBCs. Both observations suggest the role of ART in influencing the dynamic circulation of iRBCs and uRBCs. Since human spleen is well known as a "mechanical filter" that removes old and abnormal RBCs,[16] and splenic retention of artificially hardened uRBCs has been demonstrated by Buffet *et al.* using an *ex vivo* spleen,[8,32] we speculate ART induced alteration in RBC membrane stiffness and dynamic microcirculatory behavior would have a significant effect on splenic RBC filtration.[24]

Pentoxifylline, on the other hand, was initially developed to improve blood flow in the microvasculature.[39] It was suggested as a possible ancillary therapy for cerebral malaria but clinical trials showed conflicting results.[26,40] In this study, we attempted to evaluate how PTX and PTX–ART combinational therapy impact the microcirculatory behavior of RBCs infected with *P. falciparum*. The microfluidic based dynamic deformability assay with ring-stage iRBCs treated with PTX suggested a marginal albeit significant enhancement in uRBC deformability ($p < 0.05$). This result is consistent with several other deformability studies using different measurement platforms.[36,41] However, we did not observe any significant effect of PTX on iRBC deformability. Experiments with ART–PTX combinational therapy did not reveal any beneficial effect of adding PTX.

Currently the underlying molecular mechanism of ART-induced RBC stiffening is undetermined. Clinical studies revealed that the drug action is mainly attributed by the endoperoxide-bridge. Deoxyartemisinin, an artemisinin analog lacking the endoperoxide bridge, is clinically proven to be devoid of antimalarial activity,[42] indicating the important role of peroxide in artemisinin's and its derivative ART's drug action. Artesunate induced oxidative stress, a likely consequence due to its endoperoxide structure, was also suggested by Krungkrai and Yuthavong to be the key for the drug's antimalarial activity.[43] It is therefore possible that the endoperoxide-bridge could also be responsible for ART-induced RBC stiffening. This is confronted by our microfluidic experiments with iRBCs treated with deoxyartemisinin, which revealed that deoxyartemisinin has no effect on the deformability of both uRBCs and iRBCs (S2, ESI†).

It is noted that due to the complex nature of RBC deformability, different measurement tools could lead to different experimental observations. For example, prior deformability measurements by rotational ektacytometry reported that up to 4 h ART exposure would not affect uRBC deformability,[14] but our microfluidic and micropipette experiments showed significant uRBC stiffening after 2 h ART treatment. Additionally, the ektacytometry measurement suggests that ≥ 2 h ART exposure would result in a 20% reduction in the deformability separation between healthy and ring samples; our micropipette data showed that the deformability separation between uRBCs and iRBCs dropped from 0.36 to 0.18 (*i.e.* 50% drop) only at 2 h time point, and then restored back to 0.40 and 0.51, respectively, after 4 h and 6 h ART treatment. Similarly, the microfluidic system measured 14% drop (from 0.30 to 0.36) in the deformability separation only at 2 h incubation time point and the separation would then increase to 0.54 and 0.55 after 4 h and 6 h ART treatment respectively. The exact cause accounting for the discrepancies among different measurement tools remains unclear. It is likely that the difference could come from the different formulations of deformability, such as "elongation index" in ektacytometry, "membrane shear modulus" in micropipette aspiration, and "transit velocity" in microfluidics. Compared to the microfluidic and micropipette single cell measurements, ektacytometry measures bulk RBC deformability, which has an additional parameter of cell-to-cell interaction that could influence the overall result. Different shear rates were used in different systems, leading to different results due to the stress–strain (as well as the stress–strain rate) relationship.[44]

Comparing the single cell deformability results measured by microfluidic and micropipette assays the stiffening trend differs slightly, even though both systems reported decreased RBC deformability after ART treatment (Fig. 2A and 3). The microfluidic experiments showed more significant reduction in iRBC transit velocity (50%) as compared to the drop in uRBC transit velocity (10%). On the other hand micropipette aspiration displayed less differentiation in uRBC (14%) and iRBC (27%) stiffening. It is possible that the microfluidic measurement reflects the overall microcirculatory behavior of RBCs with several determining factors including RBC geometry, intracellular fluidic viscosity, as well as RBC membrane viscoelasticity,[44] whereas for the micropipette aspiration, the contribution of cell geometry and viscosity is insignificant.[45,46] Experiments measuring the size of RBCs containing 5% parasitemia (Beckman Coulter) revealed no significant change in RBC size after 6 h ART treatment (S3, ESI†), suggesting that the difference between quasi-static and dynamic RBC deformability results may be due to intracellular viscosity rather than cell size. Heme irons are believed to be actively involved in ART's selectivity.[47] Redox chemistry of RBCs is highly complicated, involving abundant hemoglobin in RBCs. Since parasites in iRBCs actively metabolize hemoglobin, and release high quantities of free heme irons, this difference may lead to differential redox-response toward ART, and possibly differentially alter the dynamic *versus* quasi-static deformability of iRBCs over uRBCs.

Our study attempted to understand the impact of drug-related changes on the ring-stage mechanical properties of *P. falciparum* iRBCs, by recreating the microcirculatory blood

flow *in vitro* using a microfluidic device, and measuring their quasi-static membrane behavior using a micropipette device. By putting iRBCs through repeated physical and mechanical barriers, compared with the quasi-static data, we were able to quantify the drug related dynamic deformability modification of iRBCs and uRBCs.

In conclusion, this work demonstrates that *in vitro* dynamic and quasi-static deformability measurements can be used to study subtle cell deformability changes resulting from various environmental factors such as *in vitro* drug treatment. ART drug treatment on malaria infected RBCs shows significantly increased RBC membrane stiffness and impaired microcirculatory deformability. Since human spleen is a ''mechanical filter'', increased RBC stiffness may enhance splenic clearance of less deformable parasite-iRBCs from the circulation.[24,32] On the other hand, the drug stimulus may also aggravate the loss of uRBCs as significant decrease in uRBC deformability was also observed *in vitro.* These hypotheses, while insightful and important, are certainly yet to be further corroborated by future *in vivo* and clinical studies. From the bioengineering perspectives, these measurements could provide a well-controlled *in vitro* experimental platform to test novel anti-malarial compounds, or clarify the drug's mode of action in relation to splenic clearance, which is generally difficult to do *in vivo* due to the lack of viable animal models and ethical considerations.

Disclosure

S. Huang, M. Diez-Silva, M. Dao, J. Han, along with others, have filed two US provisional patents based on a portion of the contents of this paper.

Acknowledgements

References

1 World Health Organization, 2010.
2 A. Trampuz, M. Jereb, I. Muzlovic and R. Prabhu, *Crit. Care*, 2003, **7**, 315–323.
3 A. G. Maier, B. M. Cooke, A. F. Cowman and L. Tilley, *Nat. Rev. Microbiol.*, 2009, **7**, 341–354.
4 A. A. Lamikanra, D. Brown, A. Potocnik, C. Casals-Pascual, J. Langhorne and D. J. Roberts, *Blood*, 2007, **110**, 18–28.
5 P. A. Buffet, I. Safeukui, G. Deplaine, V. Brousse, V. Prendki, M. Thellier, G. D. Turner and O. Mercereau-Puijalon, *Blood*, 2011, **117**, 381–392.
6 T. M. Seed and J. P. Kreier, in *Malaria, pathology, vector studies, and culture*, ed. J. P. Kreier, 1980, vol. 2, pp. 1–46.
7 A. M. Dondorp, E. Pongponratn and N. J. White, *Acta Trop.*, 2004, **89**, 309–317.
8 P. A. Buffet, G. Milon, V. Brousse, J.-M. Correas, B. Dousset, A. Couvelard, R. Kianmanesh, O. Farges, A. Sauvanet, F. Paye, M.-N. Ungeheuer, C. Ottone, H. Khun, L. Fiette, G. Guigon, M. Huerre, O. Mercereau-Puijalon and P. H. David, *Blood*, 2006, **107**, 3745–3752.
9 S. Suresh, J. Spatz, J. P. Mills, A. Micoulet, M. Dao, C. T. Lim, M. Beil and T. Seufferlein, *Acta Biomater.*, 2005, **1**, 15–30.
10 I. Safeukui, J.-M. Correas, V. Brousse, D. Hirt, G. Deplaine, S. Mulé, M. Lesurtel, N. Goasguen, A. Sauvanet, A. Couvelard, S. Kerneis, H. Khun, I. Vigan-Womas, C. Ottone, T. J. Molina, J.-M. Tré, O. Mercereau-Puijalon, G. Milon, P. H. David and P. A. Buffet, *Blood*, 2008, **112**, 2520–2528.
11 J. P. Mills, M. Diez-Silva, D. J. Quinn, M. Dao, M. J. Lang, K. S. W. Tan, C. T. Lim, G. Milon, P. H. David, O. Mercereau-Puijalon, S. Bonnefoy and S. Suresh, *Proc. Natl. Acad. Sci. U. S. A.*, 2007, **104**, 9213–9217.
12 K. Chotivanich, R. Udomsangpetch, R. McGready, S. Proux, P. Newton, S. Pukrittayakamee, S. Looareesuwan and N. J. White, *J. Infect. Dis.*, 2002, **185**, 1538–1541.
13 B. J. Angus, K. Chotivanich, R. Udomsangpetch and N. J. White, *Blood*, 1997, **90**, 2037–2040.
14 K. Chotivanich, R. Udomsangpetch, A. Dondorp, T. Williams, B. Angus, J. A. Simpson, S. Pukrittayakamee, S. Looareesuwan, C. I. Newbold and N. J. White, *J. Infect. Dis.*, 2000, **182**, 629–633.
15 P. N. Newton, K. Chotivanich, W. Chierakul, R. Ruangveerayuth, P. Teerapong, K. Silamut, S. Looareesuwan and N. J. White, *Blood*, 2001, **98**, 450–457.
16 R. E. Mebius and G. Kraal, *Nat. Rev. Immunol.*, 2005, **5**, 606–616.
17 M. Diez-Silva, Y. Park, S. Huang, H. Bow, O. Mercereau-Puijalon, G. Deplaine, C. Lavazec, S. Perrot, S. Bonnefoy, M. S. Feld, J. Han, M. Dao and S. Suresh, *Sci. Rep.*, 2012, **2**, 614.
18 M. Bessis, N. Mohandas and C. Feo, *Blood Cells*, 1980, **6**, 315–327.
19 F. C. Mokken, M. Kedaria, C. P. Henny, M. R. Hardeman and A. W. Gelb, *Ann. Hematol.*, 1992, **64**, 113–122.
20 G. B. Nash, E. Obrien, E. C. Gordonsmith and J. A. Dormandy, *Blood*, 1989, **74**, 855–861.
21 S. Chien, K. L. Sung, R. Skalak, S. Usami and A. Toezeren, *Biophys. J.*, 1978, **24**, 463–487.
22 M. Lekka, P. Laidler, D. Gil, J. Lekki, Z. Stachura and A. Z. Hrynkiewicz, *Eur. Biophys. J.*, 1999, **28**, 312–316.
23 J. P. Brody, Y. Han, R. H. Austin and M. Bitensky, *Biophys. J.*, 1995, **68**, 2224–2232.
24 H. Bow, I. V. Pivkin, M. Diez-Silva, S. J. Goldfless, M. Dao, J. C. Niles, S. Suresh and J. Han, *Lab Chip*, 2011, **11**, 1065–1073.

25 W. Graninger, F. Thalhammer and G. Locker, *J. Infect. Dis.*, 1991, **164**, 829.

26 S. Looareesuwan, P. Wilairatana, S. Vannaphan, V. Wanaratana, C. Wenisch, M. Aikawa, G. Brittenham, W. Graninger and W. H. Wernsdorfer, *Am. J. Trop. Med. Hyg.*, 1998, **58**, 348–353.

27 P. G. Kremsner, H. Grundmann, S. Neifer, K. Sliwa, G. Sahlmuller, B. Hegenscheid and U. Bienzle, *J. Infect. Dis.*, 1991, **164**, 605–608.

28 W. Trager and J. B. Jensen, *Science*, 1976, **193**, 673–675.

29 C. Lambros and J. P. Vanderberg, *J. Parasitol.*, 1979, **65**, 418–420.

30 E. Mairey, A. Genovesio, E. Donnadieu, C. Bernard, F. Jaubert, E. Pinard, J. Seylaz, J.-C. Olivo-Marin, X. Nassif and G. Duménil, *J. Exp. Med.*, 2006, **203**, 1939–1950.

31 I. C. MacDonald, D. M. Ragan, E. E. Schmidt and A. C. Groom, *Microvasc. Res.*, 1987, **33**, 118–134.

32 G. Deplaine, I. Safeukui, F. Jeddi, F. Lacoste, V. Brousse, S. Perrot, S. Biligui, M. Guillotte, C. Guitton, S. Dokmak, B. Aussilhou, A. Sauvanet, D. Cazals Hatem, F. Paye, M. Thellier, D. Mazier, G. Milon, N. Mohandas, O. Mercereau-Puijalon, P. H. David and P. A. Buffet, *Blood*, 2010, **117**, e88–e95.

33 P. A. Buffet, I. Safeukui, G. Milon, O. Mercereau-Puijalon and P. H. David, *Curr. Opin. Hematol.*, 2009, **16**, 157–164110.1097/MOH.1090b1013e32832a32831d32834b.

34 T. T. Hien, N. J. White and White, *Lancet*, 1993, **341**, 603–608.

35 D. B. Bethell, P. Teja-Isavadharm, C. X. T. Phuong, P. T. T. Thuy, T. T. T. Mai, T. T. N. Thuy, N. T. T. Ha, P. T. Phuong, D. Kyle, N. P. J. Day and N. J. White, *Trans. R. Soc. Trop. Med. Hyg.*, 1997, **91**, 195–198.

36 N. Ohshima and M. Sato, *Angiology*, 1981, **32**, 752–763.

37 B. Horvath, Z. Marton, R. Halmosi, T. Alexy, L. Szapary, J. Vekasi, Z. Biro, T. Habon, G. Kesmarky and K. Toth, *Clin. Neuropharmacol.*, 2002, **25**, 37–42.

38 D. Sinclair, S. Donegan, R. Isba and D. G. Lalloo, *Cochrane Database of Systematic Reviews 2012*, 2012, **6**.

39 B. Lell, C. Kohler, B. Wamola, C. Olola, E. Kivaya, G. Kokwaro, D. Wypij, S. Mithwani, T. Taylor, P. Kremsner and C. Newton, *Malar. J.*, 2010, **9**, 368.

40 B. K. Das, S. Mishra, P. K. Padhi, R. Manish, R. Tripathy, P. K. Sahoo and B. Ravindran, *Trop. Med. Int. Health*, 2003, **8**, 680–684.

41 T. Shimizu, E. Sekizuka, C. Oshio, K. Tsukada, T. Nagai, R. Hokari and H. Minamitani, in Engineering in Medicine and Biology Society, 1998, *Proceedings of the 20th Annual International Conference of the IEEE*, 1998, vol. 912, pp. 914–915.

42 S. R. Meshnick, T. W. Tsang, F. B. Lin, H. Z. Pan, C. N. Chang, F. Kuypers, D. Chiu and B. Lubin, *Prog. Clin. Biol. Res.*, 1989, **313**, 95–104.

43 S. R. Krungkrai and Y. Yuthavong, *Trans. R. Soc. Trop. Med. Hyg.*, **81**, 710–714.

44 S. Chien, *Annu. Rev. Physiol.*, 1987, **49**, 177–192.

45 R. M. Hochmuth, D. A. Berk and H. C. Wiles, *Ann. N. Y. Acad. Sci.*, 1983, **416**, 207–224.

46 H. Tözeren, S. Chien and A. Tözeren, *Biophys. J.*, 1984, **45**, 1179–1184.

47 S. R. Meshnick, Y. Z. Yang, V. Lima, F. Kuypers, S. Kamchonwongpaisan and Y. Yuthavong, *Antimicrob. Agents Chemother.*, 1993, **37**, 1108–1114.